

Exact entanglement renormalization for string-net models

Robert König,¹ Ben W. Reichardt,¹ and Guifré Vidal²

¹*Institute for Quantum Information, California Institute of Technology*

²*School of Physical Sciences, the University of Queensland, QLD 4072, Australia*

(Dated: March 20, 2019)

We construct an explicit renormalization group (RG) transformation for Levin and Wen’s string-net models on a hexagonal lattice. The transformation leaves invariant the ground-state “fixed-point” wave function of the string-net condensed phase. Our construction also produces an exact representation of the wave function in terms of the multi-scale entanglement renormalization ansatz (MERA). This sets the stage for efficient numerical simulations of string-net models using MERA algorithms. It also provides an explicit quantum circuit to prepare the string-net ground-state wave function using a quantum computer.

PACS numbers: 03.67.-a, 05.10.Cc, 05.30.Pr, 03.65.Vf

The study of topological phases of quantum matter has attracted much attention in recent years [1, 2, 3, 4, 5]. Experimental developments such as the discovery of the fractional quantum Hall effect have motivated the notion of topological order [1], a new type of order in extended quantum systems that is beyond the scope of Landau’s theory of symmetry-breaking phases. Topologically ordered phases exhibit a robust ground-state degeneracy and nontrivial particle statistics [1]. In particular, the collective excitations of such systems can include fermions and gauge bosons [2], even though the microscopic degrees of freedom are purely bosonic. Moreover, in two dimensions the quasi-particle excitations are anyons [3, 4]. Nonabelian anyons constitute the key ingredient for topological quantum computation, where quantum information is stored and manipulated in a way that is naturally protected against local errors [5].

Levin and Wen [6] have proposed *string-net condensation* as a mechanism underlying the formation of doubled topological phases, where it plays a role analogous to that of particle condensation in symmetry-breaking phases. Configurations of such a model are networks of strings; a doubled topological phase is obtained when the Hamiltonian favors the formation of large string-nets, with size comparable to the system size. Levin and Wen also have given a physical realization of such models as the low-energy subspace of a system with spins on a lattice and short-range interactions. Their exactly soluble “fixed-point” Hamiltonian has a scale- and topologically invariant “fixed-point” ground state. Through a heuristic reasoning, these are argued to correspond to the infrared limit of a renormalization group (RG) flow. They are therefore expected to capture the universal long distance features of all string-net condensed phases in (2+1) dimensions.

To substantiate this picture, we construct an explicit RG transformation for (2+1) dimensional string-net models such that it has the above exactly soluble models as fixed points. In this way, we contribute to establishing the “fixed-point” wave functions and Hamiltonians of Ref. [6] as the infrared limit of string-net condensed phases.

The proposed RG transformation is based on *entanglement renormalization* [7], namely on eliminating part of the ground-state entanglement before each coarse-graining step. Disentangling the system is essential in order to obtain a transformation that does not increase the local degrees of freedom of the model at each iteration. Our approach is purely algebraic, with the RG transformation being expressed in terms of the order-six tensor F_{klm}^{ijm} that characterizes the string-net model. A byproduct of the present construction is an exact description of the ground-state wave function in terms of a tensor network, the *multi-scale entanglement renormalization ansatz* (MERA) [7]. The MERA is the basis of numerical simulation algorithms for quantum systems on a 2D lattice [8] that could be used, e.g., to explore the effects of perturbing the exactly soluble string-net Hamiltonian. Finally, the MERA also provides an efficient quantum circuit that prepares the “fixed-point” wave function, thus explicitly indicating how to simulate a string-net condensed phase using a quantum computer.

Following [6], let \mathcal{G} be a trivalent graph embedded in a surface S so that the components of $S \setminus \mathcal{G}$ are simply connected (“plaquettes”). The Hilbert space $\mathcal{H}_{\mathcal{G}}$ of a *string-net model* is spanned by the different networks of labeled, oriented strings living on \mathcal{G} ’s edges. A standard basis for this space is obtained by orienting \mathcal{G} and associating to each edge e a Hilbert space $\mathcal{V}_e \cong \mathbb{C}^{N+1}$ with orthonormal basis $\{|i\rangle_e\}_{i=0}^N$. Here, i determines the type and direction of string, with $i = 0$ corresponding to the absence of a string across edge e . For each i , label i^* corresponds to a string of the same type but with the opposite direction; $0^* = 0$. Then $\mathcal{H}_{\mathcal{G}} = \bigotimes_e \mathcal{V}_e$. The model is further characterized by *branching rules*, the set of triples $\{i, j, k\}$ of string types that are allowed to come together at a vertex, e.g., $\{i, i^*, 0\}$ is always allowed. We define the *physical subspace* $\mathcal{H}_{\mathcal{G}}^{\text{phys}} \subset \mathcal{H}_{\mathcal{G}}$ as the span of all string-net configurations that have an allowed triple at every vertex.

Define a Hamiltonian $H_{\mathcal{G}}$ acting on $\mathcal{H}_{\mathcal{G}}$ by

$$H_{\mathcal{G}} = - \sum_{\text{vertices } v} Q_v - \sum_{\text{plaquettes } p} B_p . \quad (1)$$

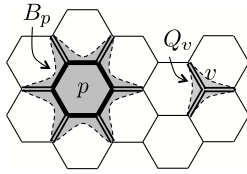


FIG. 1: Support of plaquette and vertex operators. Thick empty lines indicate those edges where the operator is diagonal in the standard basis.

Here, for each vertex v , Q_v is the projection onto the set of allowed net edge triples at v . Thus the first term projects onto $\mathcal{H}_{\mathcal{G}}^{\text{phys}}$. The second term has a more complicated definition. Let F_{klm}^{ij} be an order-six tensor, indexed by string types, satisfying certain conditions roughly described as self-consistency, unitarity and compatibility with the branching rules; see Appendix A for full details. For each plaquette p the *plaquette operator* B_p is a projection on the edges bordering p controlled by the edges with one endpoint on p (Fig. 1). More precisely, $B_p = \sum_i d_i B_p^i / \sum_i d_i^2$ where $d_i = 1/F_{ii^*0}^{ii^*0}$ and B_p^i acts on a simple plaquette p with r boundary edges as

$$B_p^i \left| \begin{array}{c} m_2 j_2 \quad m_1 j_r \quad m_r \\ j_2 \quad p \quad j_{r-1} \\ m_3 \quad \dots \quad m_{r-1} \end{array} \right\rangle = \sum_{k_1, \dots, k_n} \left(\prod_{\nu=1}^r F_{i^* k_{\nu-1} k_{\nu}^*}^{m_{\nu} j_{\nu}^* j_{\nu-1}} \right) \left| \begin{array}{c} m_2 k_1 \quad m_1 k_r \quad m_r \\ k_2 \quad p \quad k_{r-1} \\ m_3 \quad \dots \quad m_{r-1} \end{array} \right\rangle \quad (2)$$

identifying $j_0 = j_r$ and $k_0 = k_r$. The plaquette and vertex operators commute, and thus the ground space of $H_{\mathcal{G}}$ is the space simultaneously fixed by all these projections.

In Appendix A, we give a natural definition of B_p^i for more general plaquettes; roughly, B_p^i adds a loop of type i around a puncture in the center of p followed by reduction to the basis of $\mathcal{H}_{\mathcal{G}}$. Eq. (2) is a special case.

We now focus on the case where \mathcal{G} is the honeycomb lattice \mathcal{L} . Our RG transformation is a map $\mathbf{R} : \mathcal{H}_{\mathcal{L}} \rightarrow \mathcal{H}_{\tilde{\mathcal{L}}}$, where $\tilde{\mathcal{L}}$ is a coarser hexagonal lattice, that satisfies:

- (i) The physical subspace $\mathcal{H}_{\mathcal{L}}^{\text{phys}}$ is mapped into $\mathcal{H}_{\tilde{\mathcal{L}}}^{\text{phys}}$.
- (ii) Local operators on $\mathcal{H}_{\mathcal{L}}$ are mapped under conjugation by \mathbf{R} to local operators on $\mathcal{H}_{\tilde{\mathcal{L}}}$, cf. Fig. 2.

Each plaquette p of \mathcal{L} is either retained or eliminated by renormalization. We can show that the form of the plaquette part of the Hamiltonian is preserved under the map \mathbf{R} , in the following sense:

- (iii) If q is a retained plaquette of \mathcal{L} and \tilde{q} the corresponding plaquette of $\tilde{\mathcal{L}}$, then $B_q|_{\mathcal{H}_{\mathcal{L}}^0} = \mathbf{R}^\dagger B_{\tilde{q}} \mathbf{R}|_{\mathcal{H}_{\tilde{\mathcal{L}}}^0}$, where $\mathcal{H}_{\mathcal{L}}^0 \subset \mathcal{H}_{\mathcal{L}}^{\text{phys}}$ is the subspace simultaneously fixed by all B_p operators for eliminated plaquettes p .

Furthermore,

- (iv) The ground space of $H_{\mathcal{L}}$ is mapped bijectively to the ground space of $H_{\tilde{\mathcal{L}}}$. In particular, if \mathcal{L} is embedded into the plane, then the unique ground state $|\Psi\rangle_{\mathcal{L}}$ is a fixed point of \mathbf{R} .

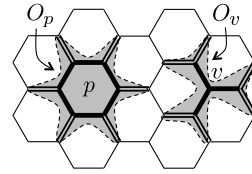


FIG. 2: Let O_p and O_v be generic operators associated with either a plaquette p or a vertex v of \mathcal{L} with support as shown (B_p and Q_v are examples). By analyzing how the supports of these operators propagate, it can be seen that \mathbf{R} maps them into operators on $\mathcal{H}_{\tilde{\mathcal{L}}}$ whose support has the same shape.

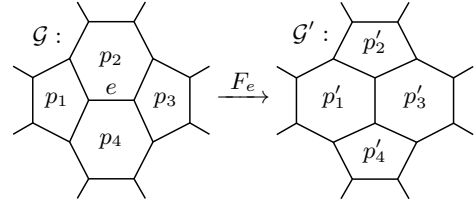


FIG. 3: An F -move reconnecting an edge e of \mathcal{G} . Plaquettes of \mathcal{G} and of \mathcal{G}' are in one-to-one correspondence.

The map \mathbf{R} is defined by a sequence of F -moves, elementary trivalent graph transformations. As shown in Fig. 3, $F_e(\mathcal{G})$ is a graph \mathcal{G}' that is the same as \mathcal{G} except with an edge e reconnected in a way that corresponds to flipping an edge in the dual graph. Using the tensor F_{klm}^{ij} , F_e also defines a linear transformation $\mathcal{H}_{\mathcal{G}} \rightarrow \mathcal{H}_{\mathcal{G}'}$, controlled by the labels $|ijkl\rangle$ of the edges adjacent to e :

$$F_e \left| \begin{array}{c} i \quad l \\ j \quad m \quad k \end{array} \right\rangle = \sum_n F_{klm}^{ijn} \left| \begin{array}{c} i \quad l \\ j \quad n \quad k \end{array} \right\rangle \quad (3)$$

in the standard string-net bases defined above. For each edge e , F_e maps $\mathcal{H}_{\mathcal{G}}^{\text{phys}}$ isomorphically to $\mathcal{H}_{\mathcal{G}'}^{\text{phys}}$, and $F_e|_{\mathcal{H}_{\mathcal{G}}^{\text{phys}}}$ can be extended to a unitary on $\mathcal{H}_{\mathcal{G}}$.

A second ingredient of \mathbf{R} are transformations that reduce the number of degrees of freedom by eliminating edges. Suppose that after some F -moves, the resulting graph \mathcal{G} contains a ‘‘tadpole,’’ i.e., a subgraph of the form shown in Fig. 4, consisting of a self-loop around

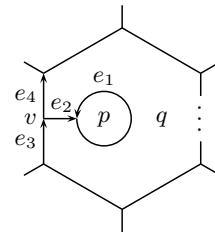


FIG. 4: When \mathcal{G} contains a tadpole around plaquette p (attached to vertex v) and the state is in the range of B_p , it is a product state with respect to the bipartition $\mathcal{G} \setminus \{e_1, e_2\} : \{e_1, e_2\}$ (Lemma 2). In this diagram, the e_i are names for the directed edges and not string-net labels.

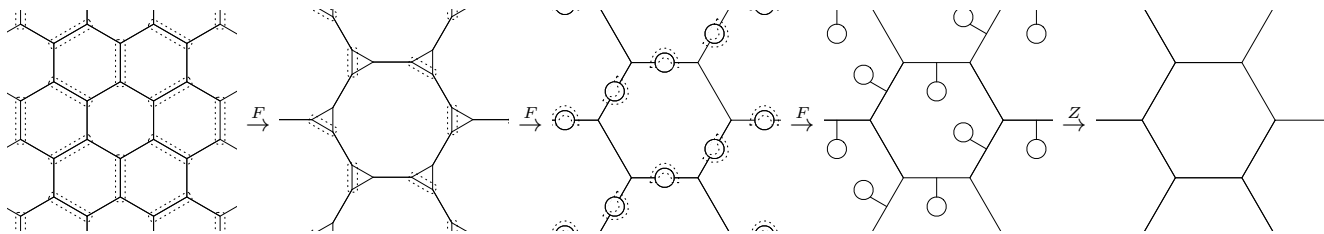


FIG. 5: The RG transformation \mathbf{R} coarse-grains lattice \mathcal{L} into $\tilde{\mathcal{L}}$. Edges where F -moves are applied are marked by dots. Note that there are many alternative sequences of moves that work equally well.

plaquette p , and three other edges. We associate with this tadpole the local operator $Z_p : \mathcal{H}_{\mathcal{G}} \rightarrow \mathcal{H}_{\mathcal{G}'}$, where \mathcal{G}' is obtained from \mathcal{G} by deleting the tadpole subgraph and replacing edges e_3, e_4 by a single edge e' :

$$Z_p = \langle \Phi |_{e_1} \otimes \langle 0 |_{e_2} \otimes \sum_i |i\rangle_{e'} \langle ii |_{e_3 e_4} \otimes \text{id}_{\mathcal{G} \setminus \{e_1, \dots, e_4\}} , \quad (4)$$

where $|\Phi\rangle = \frac{1}{\sqrt{\sum_i d_i^2}} \sum_i d_i |i\rangle$. Observe Z_p^\dagger is an isometry.

The map \mathbf{R} from the lattice \mathcal{L} into the coarser lattice $\tilde{\mathcal{L}}$ is now given by the sequence of F -moves indicated in Fig. 5, followed by eliminating the tadpoles using the Z_p maps.

The properties of the map \mathbf{R} rely on two basic claims about the behavior of plaquette operators under F -moves and the removal of tadpoles. We show that

Lemma 1. *For every edge e and plaquette p ,*

$$F_e B_p = B_{p'} F_e , \quad (5)$$

where p' corresponds to the plaquette p in the graph $\mathcal{G}' = F_e(\mathcal{G})$. Roughly speaking, F -moves “commute” with plaquette operators.

Lemma 1 implies that the plaquette part $H_{\mathcal{G}}$ is mapped to the plaquette part of $H_{\mathcal{G}'}$ under conjugation by F_e . A similar statement applies to the removal of a tadpole with head p inside a plaquette q ; this operation “commutes” with B_q provided we restrict to the subspace fixed by B_p .

Lemma 2. *Consider a tadpole around plaquette p inside a plaquette q as shown in Fig. 4, and let q' be the modified plaquette after removal of the tadpole. Then B_p is a rank-one projection,*

$$B_p = |\Phi\rangle\langle\Phi|_{e_1} \otimes |0\rangle\langle 0|_{e_2} \otimes \text{id}_{\mathcal{G} \setminus \{e_1, e_2\}} \quad (6)$$

with $|\Phi\rangle$ defined as in Eq. (4), and

$$B_q Q_v B_p = Z_p^\dagger B_{q'} Z_p . \quad (7)$$

Every ground state $|\Psi\rangle_{\mathcal{G}}$ of $H_{\mathcal{G}}$ is a product state,

$$\begin{aligned} |\Psi\rangle_{\mathcal{G}} &= Z_p^\dagger |\Psi'\rangle_{\mathcal{G}'} \\ &= |\Phi\rangle_{e_1} \otimes |0\rangle_{e_2} \otimes \left(\sum_i |ii\rangle_{e_3 e_4} \langle i |_{e'} \right) |\Psi'\rangle_{\mathcal{G}'} \end{aligned} \quad (8)$$

where $|\Psi'\rangle_{\mathcal{G}'}$ is a ground state of $H_{\mathcal{G}'}$.

Lemmas 1 and 2 can in principle be verified directly from the explicit expression (2) for the plaquette operators in terms of standard basis vectors. A simpler proof is based on the interpretation of B_p^i as adding a “virtual loop” to the surface as explained in [6, Appendix C]. The consistency of this interpretation is guaranteed by *Mac Lane’s coherence theorem* [9], which shows the required reductions yield the same result independently of the sequence of local rules applied. In terms of this interpretation, Lemma 1 is immediate since the virtual loops are added in a region that is not affected by F -moves. Similarly, Lemma 2 follows since the operator B_p effectively removes a puncture in the surface located at the center of p . Due to space constraints, we defer these details and the proofs to the appendices.

Let us now justify properties (i)-(iv) of \mathbf{R} . It is easy to check that both F -moves as well as the operators Z_p preserve the branching rule at every vertex; this proves (i). Similarly, (ii) immediately follows from the fact that \mathbf{R} is made of local operations. Statement (iii) is a direct consequence of Lemmas 1 and 2, since Eq. (7) implies $B_q |_{\mathcal{H}_{\mathcal{G}}} = Z_p^\dagger B_{q'} Z_p |_{\mathcal{H}_{\mathcal{G}'}}$.

For property (iv), note that the three rounds of F -moves in \mathbf{R} are unitaries. Therefore we only need to check that Z_p , removing a tadpole around p from a graph \mathcal{G} , is a bijection from the ground space of $H_{\mathcal{G}}$ to the ground space of $H_{\mathcal{G}'}$. Indeed, if $|\Psi\rangle_{\mathcal{G}}$ is a ground state of $H_{\mathcal{G}}$, then by Lemma 2, $|\Psi\rangle_{\mathcal{G}} = Z_p^\dagger |\Psi'\rangle_{\mathcal{G}'}$, and thus $Z_p |\Psi\rangle_{\mathcal{G}} = |\Psi'\rangle_{\mathcal{G}'}$, for some ground state $|\Psi'\rangle_{\mathcal{G}'}$ of $H_{\mathcal{G}'}$. Conversely, if $|\Psi'\rangle_{\mathcal{G}'}$ is a ground state of $H_{\mathcal{G}'}$, then let $|\Psi\rangle_{\mathcal{G}} = Z_p^\dagger |\Psi'\rangle_{\mathcal{G}'}$ so $|\Psi'\rangle_{\mathcal{G}'} = Z_p |\Psi\rangle_{\mathcal{G}}$. Eq. (7) implies that $Z_p^\dagger B_{q'} = B_q Q_v B_p Z_p^\dagger$, so $|\Psi\rangle_{\mathcal{G}} = B_q Q_v B_p |\Psi\rangle_{\mathcal{G}}$. Thus $|\Psi\rangle_{\mathcal{G}}$ is fixed by all plaquette and vertex operators, so is a ground state of $H_{\mathcal{G}}$. Alternatively, we could have used the fact that $H_{\mathcal{G}}$ and $H_{\mathcal{G}'}$ have the same ground-space degeneracy.

Let us remark that Lemmas 1 and 2 generalize considerably. In particular, Property (iii) holds even if B_q is replaced by the more general Wilson loop operators discussed in [6] that can act nontrivially on the ground space. The operator Z_p^\dagger is a special case of *surgery* between two surfaces, one of which is the sphere in this case. A version of Lemma 2 holds for general surgery.

Every iteration of the RG transformation \mathbf{R} reduces the number of sites of \mathcal{L} by one-third. In the case of a

finite system on a torus and in the ground state $|\Psi\rangle_{\mathcal{L}}$ of $H_{\mathcal{L}}$, the lattice is eventually reduced to a few edges that remain in a ground state $|\Psi\rangle_{top}$ of an effective Hamiltonian that preserves the topological features of the original model. In the terminology of entanglement renormalization [7], we can think of \mathbf{R} as being made of *disentangler*s $U : \mathcal{V}^{\otimes 5} \rightarrow \mathcal{V}^{\otimes 5}$ (the first round of F -moves) and *isometries* $W : \mathcal{V}^{\otimes 6} \rightarrow \mathcal{V}^{\otimes 3}$ (the remaining F - and Z -moves). W replaces a triangle by a single vertex. This pattern of operations has also been applied in the context of an RG transformation for classical partition functions [10]. By reversing \mathbf{R} , we obtain an explicit, logarithmic-depth quantum circuit \mathcal{C} to prepare $|\Psi\rangle_{\mathcal{L}}$ from $|\Psi\rangle_{top}$ using local gates. It is an interesting open problem whether string-net ground states can be prepared in constant quantum depth, instead of logarithmic depth.

The circuit \mathcal{C} is an exact MERA [7] of the ground-state

wave function $|\Psi\rangle_{\mathcal{L}}$ of the string-net condensed phase. As in [11], where analogous results were found for quantum double models, the MERA may now be used to numerically study, e.g., the stability of topological phases.

Acknowledgments

We thank Miguel Aguado, Lukasz Fidkowski, Alexei Kitaev, Greg Kuperberg and John Preskill for helpful conversations. R.K. and B.R. acknowledge support from NSF Grants CCF-0524828 and PHY-0456720, and ARO Grant W911NF-05-1-0294. G.V. acknowledges support from Australian Research Council (FF0668731, DP0878830).

-
- [1] X.-G. Wen, *Advances in Physics* **44**, 405 (1995). X.-G. Wen and Q. Niu, *Phys. Rev. B* **41**, 9377 (1990). X.-G. Wen, *Int. J. Mod. Phys. B* **4**, 239 (1990). X.-G. Wen, *Int. J. Mod. Phys. B* **6**, 1711 (1992).
- [2] T. Banks, R. Myerson and J.B. Kogut, *Nucl. Phys. B* **129**, 493 (1977). D. Foerster, H. B. Nielsen and M. Niomiya, *Phys. Lett. B* **94**, 135 (1980).
- [3] F. Wilczek, *Phys. Rev. Lett.* **49**, 957 (1982). D. Arovav, J. R. Schrieffer and F. Wilczek, *Phys. Rev. Lett.* **53**, 772 (1984).
- [4] A. Kitaev, *Ann. Phys.* **321**, 2 (2006).
- [5] A. Kitaev, *Ann. Phys.* **303**, 2 (2003). M. Freedman, A. Kitaev, M. Larsen and Z. Wang, *Bull. Amer. Math. Soc.* **40**, 31 (2003). C. Nayak, S. H. Simon, A. Stern, M. Freedman and S. Das Sarma, arXiv:0707.1889 (accepted to *Rev. Mod. Phys.*).
- [6] M. A. Levin and X.-G. Wen, *Phys. Rev. B* **71**, 045110 (2005).
- [7] G. Vidal, *Phys. Rev. Lett.* **99**, 220405 (2007). G. Vidal, arXiv:quant-ph/0610099.
- [8] G. Evenbly and G. Vidal, arXiv:0710.0692. L. Cincio, J. Dziarmaga and M. M. Rams, *Phys. Rev. Lett.* **100**, 240603 (2008). G. Evenbly and G. Vidal, arXiv:0801.2449.
- [9] S. Mac Lane, *Categories for the working mathematician*, Springer, 2nd ed., (1998).
- [10] M. Levin and C. P. Nave, *Phys. Rev. Lett.* **99**, 120601 (2007), arXiv:cond-mat/0611687.
- [11] M. Aguado and G. Vidal, *Phys. Rev. Lett.* **100**, 070404 (2008).

APPENDIX A: BASIC DEFINITIONS FOR GENERAL STRING-NET MODELS

We first review the properties that the tensor F_{kln}^{ijm} needs to satisfy in order to define a string-net model. Start by encoding the branching rules into a tensor δ_{ijk} , with $\delta_{ijk} = 1$ if string types i, j, k are allowed to come together at a vertex, and $\delta_{ijk} = 0$ otherwise. The branch-

ing rules are assumed to satisfy $\delta_{ij^*0} = \delta_{ij}$, where δ_{ij} is the Kronecker delta. Assume that the F tensor satisfies for all i, j, \dots, s :

$$\text{physicality: } F_{kln}^{ijm} \delta_{ijm} \delta_{klm^*} = F_{kln}^{ijm} \delta_{iln} \delta_{jkn^*} \quad (\text{A1})$$

$$\text{pentagon identity: } \sum_{n=0}^N F_{kpn}^{mlq} F_{mns}^{jip^*} F_{lkr}^{jns} = F_{q^*kr}^{jip^*} F_{mls}^{r^*iq^*} \quad (\text{A2})$$

$$\text{unitarity: } (F_{kln}^{ijm})^* = F_{k^*l^*n^*}^{i^*j^*m^*} \quad (\text{A3})$$

$$\text{tetrahedral symmetry: } F_{kln}^{ijm} = F_{lkn^*}^{jim} = F_{jin}^{lkm^*} = F_{k^*nl}^{imj} \sqrt{\frac{d_m d_n}{d_j d_i}} \quad (\text{A4})$$

$$\text{normalization: } F_{j^*jk}^{ii^*0} = \sqrt{\frac{d_k}{d_i d_j}} \delta_{ijk} \quad (\text{A5})$$

where $d_i^{-1} = F_{ii^*0}^{ii^*0} \neq 0$. Then via Eqs. (1), (2) and

$$Q_v = \sum_{i,j,k} \delta_{ijk} \left| \begin{array}{c} i \\ j \quad \vee \quad k \\ v \end{array} \right| \left| \begin{array}{c} i \\ j \quad \wedge \quad k \\ v \end{array} \right|, \quad (\text{A6})$$

the tensor F_{kln}^{ijm} gives rise to a Hamiltonian $H_{\mathcal{L}}$ of a string-net model on the honeycomb lattice \mathcal{L} [6]. To define $H_{\mathcal{G}}$ for more general trivalent graphs \mathcal{G} , though, we need to extend the definition (2) of the operators B_p^i to arbitrary plaquettes.

Recall that \mathcal{G} is embedded in a surface S . Put a puncture in the interior of each plaquette of \mathcal{G} , and let S^* be the resulting punctured surface. A *smooth string net* is an equivalence class of directed trivalent graphs embedded in S^* , where the edges carry string labels (cf. [6, Appendix C] for the case of the honeycomb lattice). The equivalences consist of isotopy, i.e., smooth deformations of the embedding in S^* (for example, crossing punctures is not allowed), and of reversing the direction of an edge labeled i while changing the label to i^* .

Any smooth string net representative embedded in $\mathcal{G} \subset S^*$ can be associated with one of the basis vectors of $\mathcal{H}_{\mathcal{G}} = \bigotimes_e \mathcal{V}_e$ in the natural way, assigning $|0\rangle$ for any edge not crossed by the smooth string net. More

generally, every smooth string net on S^* uniquely determines an element of $\mathcal{H}_{\mathcal{G}}$ by applying some sequence of the following local substitution rules to obtain a linear combination of smooth string nets in \mathcal{G} :

$$\begin{array}{c} \text{---} i \text{---} \\ \text{---} j \text{---} \end{array} = \begin{array}{c} \text{---} i \text{---} \\ \text{---} j \text{---} \\ \text{---} 0 \text{---} \end{array} \quad (\text{A7})$$

$$\begin{array}{c} \text{---} i \text{---} \\ \text{---} i \text{---} \end{array} = d_i \quad (\text{A8})$$

$$\begin{array}{c} \text{---} i \text{---} \\ \text{---} k \text{---} \\ \text{---} l \text{---} \\ \text{---} j \text{---} \end{array} = \delta_{ij} \begin{array}{c} \text{---} i \text{---} \\ \text{---} k \text{---} \\ \text{---} l \text{---} \\ \text{---} j \text{---} \end{array} \quad (\text{A9})$$

$$\begin{array}{c} \text{---} i \text{---} \\ \text{---} m \text{---} \\ \text{---} j \text{---} \\ \text{---} k \text{---} \end{array} = \sum_n F_{kln}^{ijm} \begin{array}{c} \text{---} i \text{---} \\ \text{---} l \text{---} \\ \text{---} j \text{---} \\ \text{---} k \text{---} \\ \text{---} n \text{---} \end{array} \quad (\text{A10})$$

Crucially, the element of $\mathcal{H}_{\mathcal{G}}$ obtained in this fashion is independent of which sequence of local rules was applied. This self-consistency of the local rules is a special case of Mac Lane's coherence theorem [9] (see also [4, Appendix E]).

Now define B_p^i as adding a counterclockwise oriented loop with label i around the puncture in p , followed by reduction back to the standard basis of $\mathcal{H}_{\mathcal{G}}$. It is straightforward to derive Eq. (2) from this more general definition (Example 2). This completes the definition of $H_{\mathcal{G}}$ for general trivalent graphs \mathcal{G} .

Example 1. A smooth string-net "bubble" with three incoming edges and no interior punctures can be simplified to a trivalent vertex by, e.g., applying an F -move to the edge labeled l , using Eqs. (A10) and (A9), followed by applying an F -move to the edge labeled m and simplifying with Eqs. (A9), (A8) and (A5):

$$\begin{array}{c} \text{---} k \text{---} \\ \text{---} n \text{---} \\ \text{---} m \text{---} \\ \text{---} l \text{---} \\ \text{---} i \text{---} \\ \text{---} j \text{---} \end{array} = F_{jm^*k^*}^{nil^*} \begin{array}{c} \text{---} k \text{---} \\ \text{---} n \text{---} \\ \text{---} m \text{---} \\ \text{---} i \text{---} \\ \text{---} j \text{---} \end{array} \quad (\text{A11})$$

$$= \sqrt{\frac{d_m d_n}{d_k}} \delta_{ijk} F_{jm^*k^*}^{nil^*} \begin{array}{c} \text{---} k \text{---} \\ \text{---} i \text{---} \\ \text{---} j \text{---} \end{array}$$

Example 2. The operator B_p^i adds a loop of type i , followed by expanding the resulting smooth string net into a sum of standard basis vectors. For example,

$$\begin{array}{c} \text{---} m_3 \text{---} \\ \text{---} j_3 \text{---} \\ \text{---} j_2 \text{---} \\ \text{---} m_2 \text{---} \\ \text{---} j_1 \text{---} \\ \text{---} m_1 \text{---} \end{array} = \sum_{k_1, k_2, k_3} \prod_{\nu=1}^3 F_{j_\nu^* k_\nu^*}^{i^* i_0} \begin{array}{c} \text{---} m_3 \text{---} \\ \text{---} j_3 \text{---} \\ \text{---} j_2 \text{---} \\ \text{---} k_2 \text{---} \\ \text{---} i \text{---} \\ \text{---} i \text{---} \\ \text{---} j_1 \text{---} \\ \text{---} k_1 \text{---} \\ \text{---} m_1 \text{---} \end{array}$$

$$= \sum_{k_1, k_2, k_3} \left(\prod_{\nu=1}^3 F_{i^* k_{\nu-1}^*}^{m_\nu j_\nu^* j_{\nu-1}^*} \right) \begin{array}{c} \text{---} m_3 \text{---} \\ \text{---} k_3 \text{---} \\ \text{---} k_2 \text{---} \\ \text{---} i \text{---} \\ \text{---} k_1 \text{---} \\ \text{---} m_1 \text{---} \end{array}$$

Here in the first step we have applied three F -moves, and in the second step we have applied Eq. (A11) three times and simplified. The puncture in plaquette p is marked by \times . Thus we have derived Eq. (2) for the case that p has $r = 3$ sides.

Remark. The derivation in Example 2 suggests a convenient shorthand rule for determining the action of B_p^i . First, draw a loop with label i going counterclockwise along the boundary inside plaquette p . Then, formally replace each T -junction as shown:

$$\begin{array}{c} \text{---} a \text{---} \\ \text{---} b \text{---} \\ \text{---} c \text{---} \\ \text{---} i \text{---} \end{array} \longrightarrow F_{i^* c' b'}^{abc} \begin{array}{c} \text{---} a \text{---} \\ \text{---} b' \text{---} \\ \text{---} c' \text{---} \end{array}$$

Finally, identify primed variables at adjacent junctions, and sum over the remaining primed variables. It is easy to check that this rule computes B_p^i , although special care must be taken to apply the rule to a plaquette with degenerate boundary.

APPENDIX B: PROOFS OF LEMMAS 1 AND 2

Proof of Lemma 1. We claim that $F_e B_p^i = B_p^i F_e$. Since B_p^i is defined as adding a loop of type i followed by reduction to the standard basis of the graph, this claim is equivalent to the following diagram commuting:

$$\begin{array}{ccccc} \begin{array}{c} \text{---} \dots \text{---} \\ \text{---} \times p \text{---} \\ \text{---} e \text{---} \end{array} & \xrightarrow{\text{Add loop of type } i} & \begin{array}{c} \text{---} \dots \text{---} \\ \text{---} \times \text{---} \\ \text{---} i \text{---} \end{array} & \xrightarrow{\text{Reduce to } \mathcal{H}_{\mathcal{G}}} & \begin{array}{c} \text{---} \dots \text{---} \\ \text{---} \times \text{---} \end{array} \\ \downarrow F_e & & \downarrow F_e & & \downarrow F_e \\ \begin{array}{c} \text{---} \dots \text{---} \\ \text{---} \times \text{---} \end{array} & \xrightarrow{\text{Add loop of type } i} & \begin{array}{c} \text{---} \dots \text{---} \\ \text{---} \times \text{---} \\ \text{---} i \text{---} \end{array} & \xrightarrow{\text{Reduce to } \mathcal{H}_{\mathcal{G}'}} & \begin{array}{c} \text{---} \dots \text{---} \\ \text{---} \times \text{---} \end{array} \end{array}$$

To simplify the diagram, we have drawn only \mathcal{G} and $\mathcal{G}' = F_e(\mathcal{G})$, instead of writing superpositions of basis states.

Now the left half of this diagram commutes since e is separated away from the puncture. The right half of the diagram commutes by Mac Lane's coherence theorem, since the two ways around it are different ways of reducing to $\mathcal{H}_{\mathcal{G}'}$. \square

Thus Lemma 1 is a nearly immediate corollary of Mac Lane's coherence theorem. This simple proof shows the usefulness of defining B_p^i using smooth string nets. A similar argument shows that $[B_p^i, B_q^j] = 0$ for all plaquettes p, q and all string-net types i, j , as we asserted below Eq. (2).

For the proof of Lemma 2, we first show the following rule that applies to smooth string nets:

Lemma 3.

$$B_p \begin{array}{c} \uparrow i \\ \times p \end{array} = B_p \begin{array}{c} i \\ \times \end{array} \quad (\text{B1})$$

Intuitively, Lemma 3 says that applying B_p effectively removes from S^* the puncture p by allowing strings to be carried over it isotopically. The proof is by applying two F -moves. Let $\mathcal{D} = \sqrt{\sum_k d_k^2}$, the ‘‘total quantum dimension.’’

Proof. By definition of B_p ,

$$\begin{aligned} \mathcal{D}^2 B_p \begin{array}{c} \uparrow i \\ \times p \end{array} &= \sum_j d_j B_p^j \begin{array}{c} \uparrow i \\ \times p \end{array} \\ &= \sum_j d_j \begin{array}{c} \uparrow i \\ \times j \end{array} \\ &= \sum_{j,k} d_j F_{j^* j k}^{i^* i 0} \begin{array}{c} i \\ \times j \end{array} \\ &= \sum_{j,k} \sqrt{\frac{d_j d_k}{d_i}} \delta_{i^* j k} \begin{array}{c} i \\ \times j \end{array} \end{aligned}$$

We have made an F -move and used Eq. (A5). Every smooth string net depicted above represents the corresponding element of $\mathcal{H}_{\mathcal{G}}$; the use of Mac Lane’s theorem is implicit. Now by symmetry,

$$\begin{aligned} \sum_{j,k} \sqrt{\frac{d_j d_k}{d_i}} \delta_{i^* j k} \begin{array}{c} i \\ \times j \end{array} &= \sum_k d_k \begin{array}{c} i \\ \times k \end{array} \\ &= \mathcal{D}^2 B_p \begin{array}{c} \times \\ i \end{array} \quad \square \end{aligned}$$

Proof of Lemma 2. First, note that

$$\begin{aligned} B_p \begin{array}{c} j \\ \times p \end{array} &= B_p \begin{array}{c} j \\ \times p \end{array} \\ &= \delta_{j0} B_p \begin{array}{c} k \\ \times p \end{array} \\ &= \delta_{j0} d_k B_p \times p \\ &= \delta_{j0} \frac{d_k}{\mathcal{D}} |\Phi\rangle_{e_1} \otimes |0\rangle_{e_2} \quad (\text{B2}) \end{aligned}$$

where we have applied Lemma 3, and Eqs. (A8) and (A9). Eq. (6) follows since B_p is a projection.

Now we can argue that $B_q^i Q_v B_p = Z_p^\dagger B_{q'}^i Z_p$, from which Eq. (7) follows. On the left-hand side we know from (6) and (B2)

$$Q_v B_p = |\Phi\rangle\langle\Phi|_{e_1} \otimes |0\rangle\langle 0|_{e_2} \otimes \sum_i |ii\rangle\langle ii|_{e_3 e_4}$$

$$= \mathcal{D} B_p |0\rangle\langle\Phi|_{e_1} \otimes |0\rangle\langle 0|_{e_2} \otimes \Delta^\dagger \Delta$$

where $\Delta = \sum_j |j\rangle_{e'} \langle jj|_{e_3, e_4}$. Similarly, we have

$$Z_p^\dagger B_{q'}^i Z_p = \mathcal{D} B_p \Delta^\dagger B_{q'}^i \Delta \otimes |0\rangle\langle\Phi|_{e_1} \otimes |0\rangle\langle 0|_{e_2} .$$

Thus we need only verify that $B_p B_{q'}^i \Delta^\dagger \Delta \otimes |00\rangle_{e_1 e_2} = B_p |00\rangle_{e_1 e_2} \otimes \Delta^\dagger B_{q'}^i \Delta \otimes |00\rangle_{e_1 e_2}$. Indeed, letting $\text{red}_{\mathcal{G}}$ (resp. $\text{red}_{\mathcal{G}'}$) mean reducing the smooth string net to $\mathcal{H}_{\mathcal{G}}$ (resp. $\mathcal{H}_{\mathcal{G}'}$),

$$\begin{aligned} &B_p B_{q'}^i (\text{id}_{\mathcal{G} \setminus \{e_3, e_4\}} \otimes \Delta^\dagger \Delta) |00jj\rangle_{e_1 e_2 e_3 e_4} \\ &= B_p \begin{array}{c} j \\ 0 \quad i \\ \times p \quad \times q \end{array} \\ &= B_p \text{red}_{\mathcal{G}} \begin{array}{c} i \\ \times p \quad \times q \end{array} \\ &= B_p |00\rangle_{e_1 e_2} \otimes \Delta^\dagger \text{red}_{\mathcal{G}'} \begin{array}{c} i \\ \times q' \end{array} \\ &= B_p (|00\rangle_{e_1 e_2} \otimes \Delta^\dagger B_{q'}^i \Delta |jj\rangle_{e_3 e_4}) \end{aligned}$$

where the first and last equalities are by definition of B_q^i and $B_{q'}^i$, the second equality is by Lemma 2, and the third equality is because the exact same sequence of steps can be used to reduce the pictured smooth string net to $\mathcal{H}_{\mathcal{G}}$ as can be used to reduce it to $\mathcal{H}_{\mathcal{G}'}$. Eq. (8) now follows immediately. \square

Finally, in Fig. 6, we display the different ways that local operators O_p or O_v , as specified in Fig. 2 can propagate under the map \mathbf{R} .

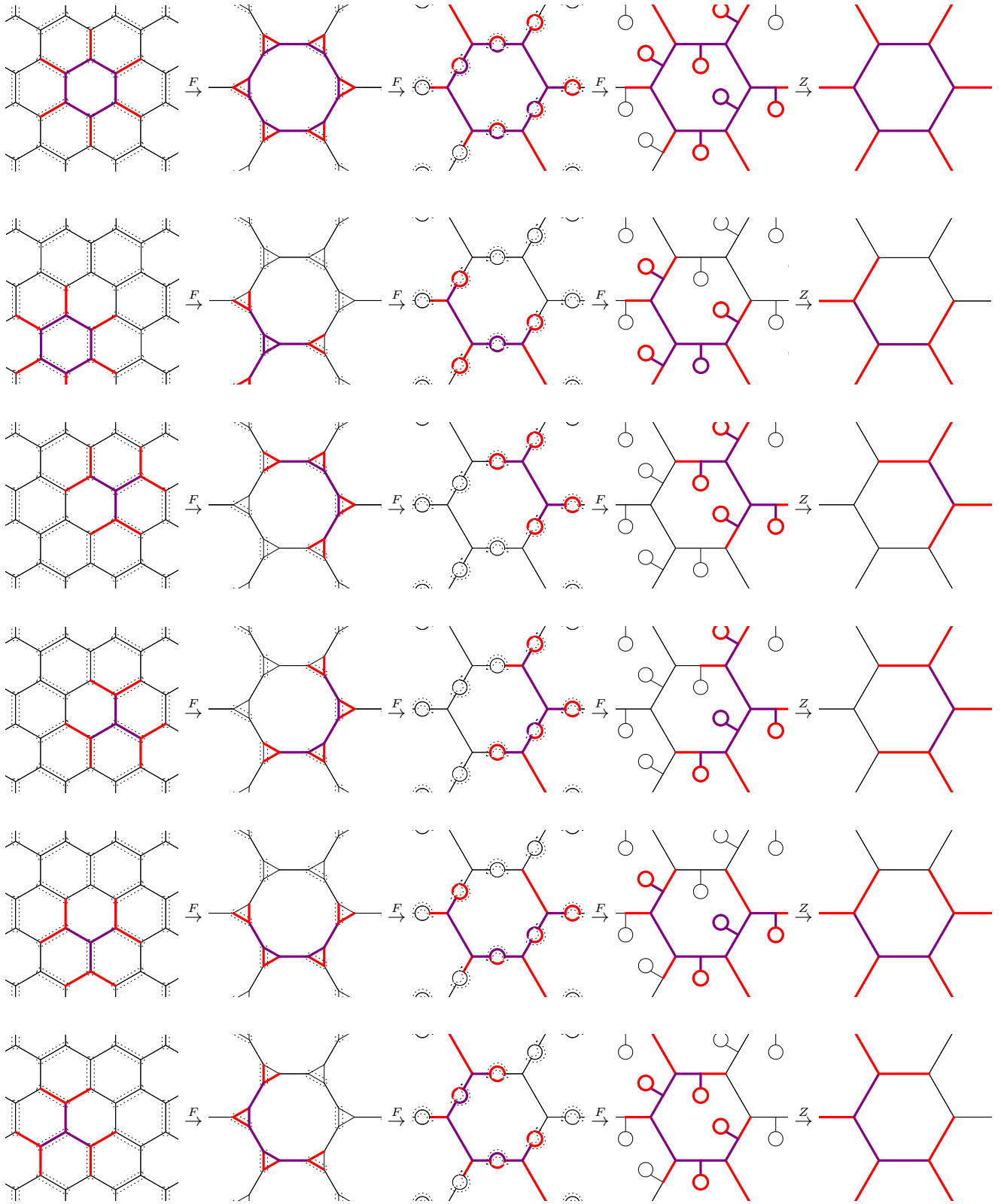


FIG. 6: Propagation of the local operators O_p (first two cases) or O_v (remaining four cases) under the RG transformation \mathbf{R} . See Fig. 2. In each case, colored edges mark spins on which the operator is supported; on the red edges, the operator is diagonal in the standard basis.